

Supporting Information

**Preservation of High-Pressure Synthesizes
Pentazolate Anions *Cyclo-N₅* Confined in *Sp³*-
hybridized Boron Nitride**

Linlin Guo ^b, Shuang Liu ^a, Yuanyuan Liu ^a, Xu Guo ^a, Zitong Zhao ^a, Minghong Sui ^a,
Ran Liu ^a, Bo Liu ^a, Thomas Wågberg ^c, Hamid Reza Barzegar ^c, Qing Liang ^d, Wei
Zhang ^d, Ying Zhang ^{a, *}, Zhen Yao^{a, *}, Peng Wang ^{a, *}

^a State Key Laboratory of High Pressure and Superhard Materials, Jilin University,
Changchun, 130012, China

^b Institute of Light Resources and Environmental Sciences, Henan Academy of
Sciences, Zhengzhou, 460000, China

^c Department of Physics, Umeå University, Umeå, Sweden

^d Key Laboratory of Automobile Materials MOE, and School of Materials Science &
Engineering, and Electron Microscopy Center, Jilin University, Changchun, 130012
China

Content

1. Supplement Figures and Tables..	2
2. Refferences.....	8

1. Supplement Figures and Tables.

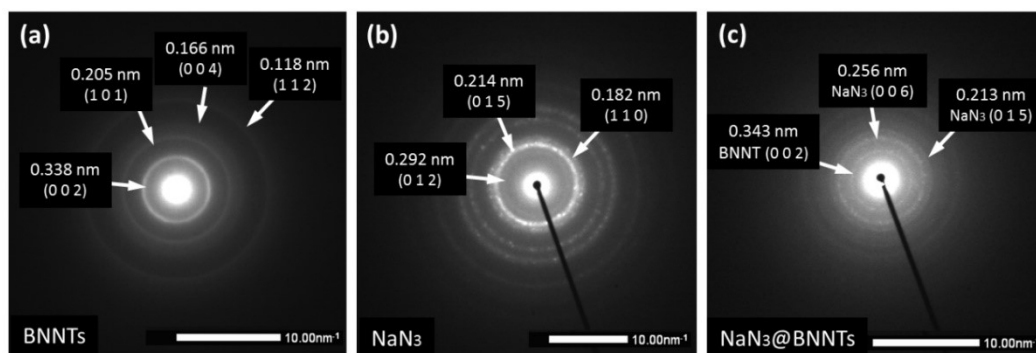


Figure S1. The SAED pattern of (a) BNNTs, (b) NaN₃ and (c) NaN₃@BNNTs.

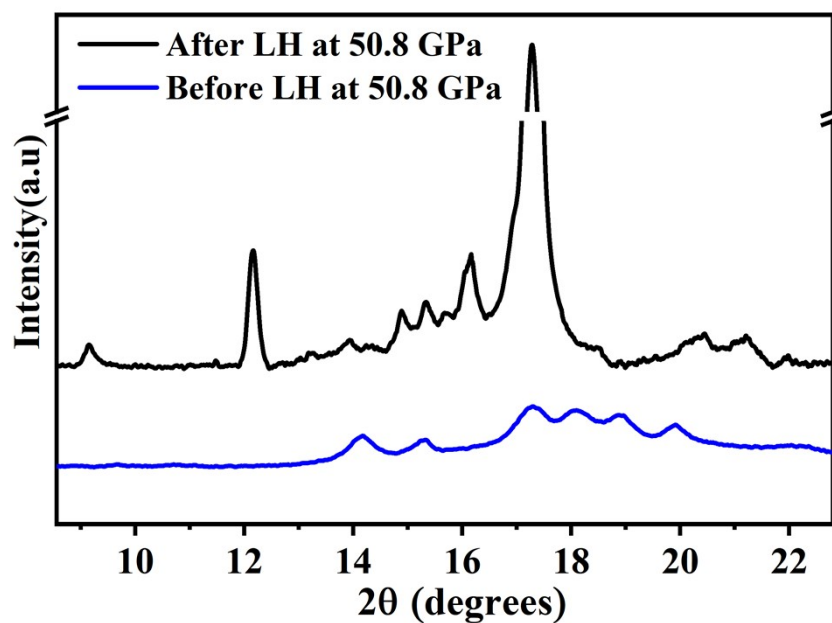


Figure S2. Experimental XRD patterns of NaN₃@MWBNTs sample at 50.8 GPa before laser heating (LH) (blue curve) and of confined pentazole sodium after LH (black curve).

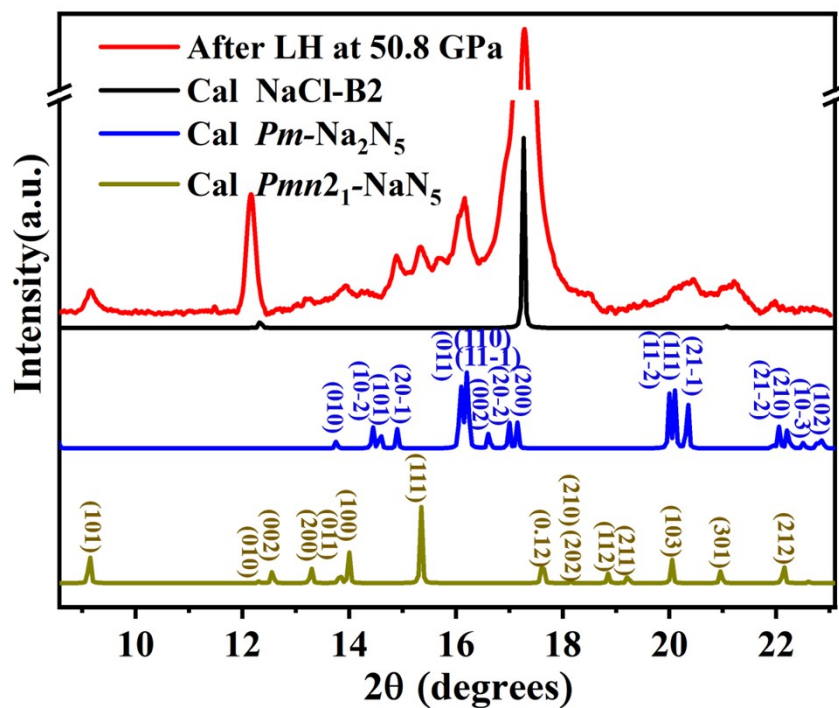


Figure S3. X-ray diffraction patterns of the confined sample taken at 50.8 GPa after laser heating (LH) compared to the calculated XRD pattern of the theoretical $Pmn2_1\text{-NaN}_5$, $Pm\text{-Na}_2\text{N}_5$ and NaCl-B2 crystal structure.

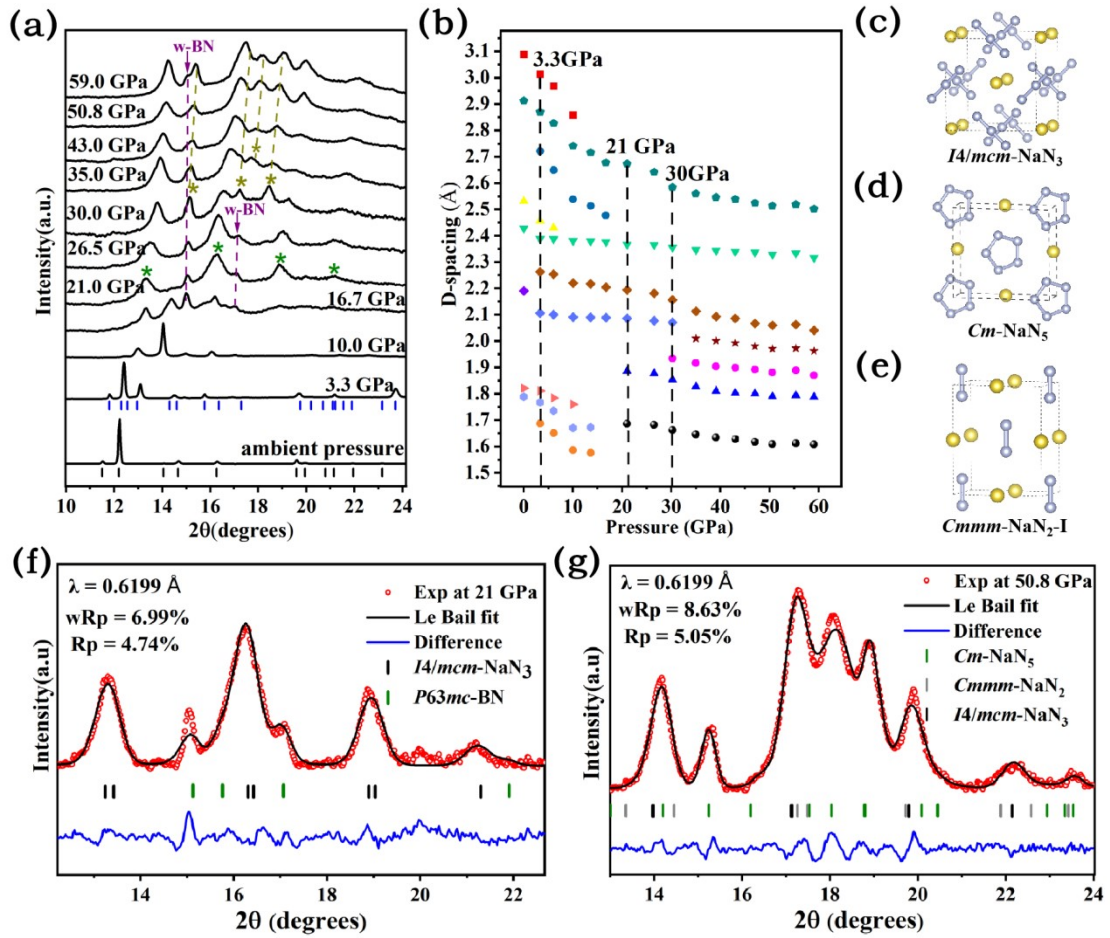


Figure S4. (a) Cold-compression experiments XRD patterns of NaN₃@MWBNTs up to 59.0 GPa. Vertical black and blue ticks mark Bragg peaks positions of *R-3m*-NaN₃ and *C2/m*-NaN₃ respectively. The green and yellow asterisks mark represents the diffraction peaks of *I4/mcm*-NaN₃ and *Cm*-NaN₅, respectively. The yellow and purple dash lines represented are guides for the diffraction peaks of *Cm*-NaN₅ and *w-BN*. (b) The d-spacing variation under pressure of confined sample at room temperature. The black dash lines represents the phase transition pressure observed in the Cold-compression experiments. The crystal structure of the (c) *I4/mcm*-NaN₃, (d) *Cm*-NaN₅, and (e) *Cmmm*-NaN₂-I. Le Bail refinement of integrated X-ray diffraction pattern obtained from the confined sample at (f) 21 GPa and (g) 50.8 GPa.

Cold-compression experiments of NaN₃@MWBNTs were performed up to 59.0 GPa at room temperature (Figure S2a). At ambient pressure, NaN₃ confined in MWBNTs shows a typical rhombohedral structure with *R-3m* space group

symmetry (ICSD #1144). Le Bail refinement of the experimental XRD pattern was performed for the confined NaN_3 and the lattice parameters were provided (Table S1). Phase transition from $R\text{-}3m\text{-NaN}_3$ to $C2/m\text{-NaN}_3$ was observed at 3.3 GPa. Above 16.7 GPa, two diffraction peaks appeared at ~ 15 and 17° (masked by purple dash lines), which can be attributed to the (100) and (002) reflections in w-BN ²⁻⁴. Then at 21.0 GPa, the diffraction peaks of $C2/m\text{-NaN}_3$ disappear gradually and four new peaks appear (marked by green asterisks), indicating the second phase transition from monoclinic $C2/m\text{-NaN}_3$ to tetragonal $I4/mcm\text{-NaN}_3$ (Figure S2c and f) ⁵. With compressing to 30-35 GPa, three diffraction peaks of $I4/mcm\text{-NaN}_3$ (around 16.34 , 19.01 , and 21.19°) become much weaker and four new diffraction peaks appear (marked by yellow asterisks). Le-Bail fits of the diffraction pattern at 50.8 GPa (Figure S2g) indicating that under cold compression, the confined $I4/mcm\text{-NaN}_3$ begins to partially transform above 30.0 GPa, yielding a mixture of $Cm\text{-NaN}_5$ and $Cmmm\text{-NaN}_2$ (Figure S2d and e), as Zhou et al. Reported ⁶. This three-phase coexistence ($I4/mcm\text{-NaN}_3$, $Cm\text{-NaN}_5$, and $Cmmm\text{-NaN}_2$) persists throughout the compression process up to our maximum pressure of 59.0 GPa. The crystallographic data of $Cmmm\text{-NaN}_2$ and $Cm\text{-NaN}_5$ unit cells at 50.8 GPa are listed in Table S2.

During the compress process, the sp^3 -bonded w-BN capsule with super hardness and strength act as a pressure shield, increasing the phase transition pressures of NaN_3 . Zhou et al. reported two phase transitions in NaN_3 : (1) from $C2/m\text{-NaN}_3$ to $I4/mcm\text{-NaN}_3$ at 15.5 GPa, and (2) $I4/mcm\text{-NaN}_3$ to $Cm\text{-NaN}_5$ and $Cmmm\text{-NaN}_2$ above 19.6 GPa ⁶. In contrast, our work reveals that under confinement, the phase transitions occur at notably higher pressures: the $C2/m \rightarrow I4/mcm$ transition shifts to 21 GPa, and the $I4/mcm \rightarrow Cm + Cmmm$ transition occurs at 30 GPa. This represents a substantial pressure increase of 5.5 GPa and 10.4 GPa, respectively, compared to the unconfined sample, demonstrating the significant confinement effect of sp^3 -hybridized BN encapsulation under high pressure.

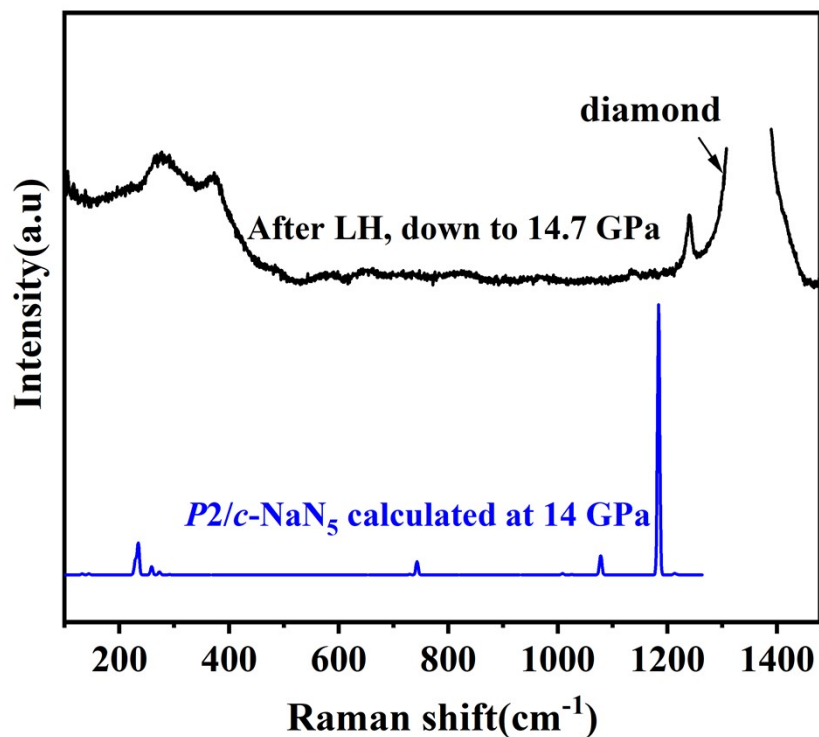


Figure S5. Experimental Raman spectrum of the laser-heated sample down to 14.7 GPa (black curve) compared with theoretical Raman spectra of $P2/c\text{-NaN}_5$ (blue line) at 14 GPa.

Table S1. Lattice constant for the pure NaN_3 and confined NaN_3 under ambient condition.

	Space group	a=b (Å)	c (Å)	V (Å ³)
NaN_3(ICSD #1144)	R-3m	3.646(0)	15.223(0)	175.2(5)
Confined NaN_3	R-3m	3.639(1)	15.207(8)	174.4(2)

Table S2. Crystallographic Data for the $I4/mcm$ -NaN₃, $Cmmm$ -NaN₂, Cm -NaN₅, obtained from our experiments and Ref.38.

	$I4/mcm$ -NaN ₃		$Cmmm$ -NaN ₂		Cm -NaN ₅	
Pressure	50.8 GPa	57.9 GPa	50.8 GPa	57.9 GPa	50.8 GPa	57.9 GPa
	This work	Ref.38	This work	Ref.38	This work	Ref.38
a (Å)	5.102(3)	5.021(3)	4.130(1)	4.078(1)	6.210(7)	6.167(4)
b (Å)	5.102(3)	5.021(2)	4.929(7)	4.854(4)	5.471(7)	5.345(1)
c (Å)	5.092(1)	5.012(2)	2.668(1)	2.621(1)	2.922(8)	2.871(2)
β (deg)	90	90	90	90	78.112(1)	78.07(2)

Table S3. Crystallographic Data for the $Pmn2_1$ -NaN₅, Pm -Na₂N₅ and $P2/c$ -NaN₅ obtained from our experiments and calculations..

	$Pmn2_1$ -NaN ₅		Pm -Na ₂ N ₅		$P2/c$ -NaN ₅	
Pressure	50.8 GPa	Cal. 50 GPa	50.8 GPa	Cal. 50 GPa	14.7 GPa	Cal. 15 GPa
a (Å)	5.359(3)	5.440(1)	4.779(5)	4.645(6)	7.631(1)	7.862(2)
b (Å)	2.891(4)	2.847(5)	2.588(1)	2.595(1)	4.912(3)	5.121(5)
c (Å)	5.665(7)	5.671(8)	4.935(6)	4.811(8)	5.750(5)	5.947(6)
β (deg)	90	90	90	90	147.874(4)	149.580(6)

2. Refferencs.

- (1) Fathalizadeh, A.; Pham, T.; Mickelson, W.; Zettl, A. Scaled Synthesis of Boron Nitride Nanotubes, Nanoribbons, and Nanococoons Using Direct Feedstock Injection into an Extended-Pressure, Inductively-Coupled Thermal Plasma. *Nano. Lett.* **2014**, *14*, 4881.
- (2) Muthu, D. V. S.; Midgley, A. E.; Petruska, E. A.; Sood, A. K.; Bando, Y.; Golberg, D.; Kruger, M. B. High-pressure effects on boron nitride multi-walled nanotubes: An X-ray diffraction study. *Chem. Phys. Lett.* **2008**, *466*, 205-208.
- (3) Dong, Z.; Song, Y. Transformations of cold-compressed multiwalled boron nitride nanotubes probed by infrared spectroscopy. *J. Phys. Chem. C.* **2010**, *114*, 1782-1788.
- (4) Ji, C.; Levitas, V. I.; Zhu, H.; Chaudhuri, J.; Marathe, A.; Ma, Y. Shear-induced phase transition of nanocrystalline hexagonal boron nitride to wurtzitic structure at room temperature and lower pressure. *PNAS.* **2012**, *109*, 19108-19112.
- (5) Zhu, H.; Zhang, F.; Ji, C.; Hou, D.; Wu, J.; Hannon, T.; Ma, Y. Pressure-induced series of phase transitions in sodium azide. *J. Appl. Phys.* **2013**, *113*, 033511.
- (6) Zhou, M.; Liu, S.; Du, M.; Shi, X.; Zhao, Z.; Guo, L.; Liu, B.; Liu, R.; Wang, P.; Liu, B. High-pressure-induced structural and chemical transformations in NaN_3 . *J. Phys. Chem. C.* **2020**, *124*, 19904-19910.